

# YSZ/Ni–YSZ semi-cells shaped by electrophoretic deposition

P. García, B. Ferrari\*, R. Moreno, A.J. Sánchez-Herencia, M.T. Colomer

*Instituto de Cerámica y Vidrio, CSIC, c/Kelsen no. 5, 28049 Madrid, Spain*

Available online 3 April 2007

## Abstract

The manufacturing of Ni/YSZ self-supported films by aqueous electrophoretic deposition (EPD) for fuel cell applications is reported. The amount and the additives used in an aqueous suspension of Ni and YSZ powders have been optimized to obtain homogeneous and crack-free Ni/YSZ films on graphite substrates. Formed deposits are treated in air at 800 °C for graphite burning out and further sintered in reducing N<sub>2</sub>/10 vol.% H<sub>2</sub> atmosphere at 1200 °C. Self-supported films with a gradient function in composition were shaped as a semi-cell in a single-step process without the use of other alternative shaping methods.

© 2007 Elsevier Ltd. All rights reserved.

*Keywords:* Suspension; Shaping; Fuel cell; YSZ

## 1. Introduction

Solid oxide fuel cells (SOFCs) have attracted great attention as a new electric power generation system because of their high energy conversion efficiency and excellent long-term stability.<sup>1</sup> Therefore, various shaping processes have been adopted for preparing SOFCs, especially thin electrolytes.<sup>2</sup> EPD is a coating technique using an electrochemical driving force and its application in SOFCs is expected to have some advantages<sup>3,4</sup>: single coatings or laminate can be made in any shape (for planar or tubular configurations), either porous or dense. EPD allows to simplify manufacturing of SOFC stacks with complex design and significant cost reduction.

Some published works describe the EPD of either anode supported electrolytes or cathode supported ones. The fabrication of complete cells alternating different processes and intermediate thermal treatments has been also reported.<sup>4–6</sup> These studies generally describe the shaping by EPD of an YSZ thin film, using a porous substrate shaped before by other methods. This work deals with the manufacture of Ni–YSZ/YSZ self-supported semi-cells by aqueous EPD in a single-step process.

## 2. Experimental

Nickel (Nickel 210H, INCO, Canada) and cubic ZrO<sub>2</sub> stabilized with 8 mol% Y<sub>2</sub>O<sub>3</sub> (8YSZ, TOSOH, Japan) submicronic

powders, with mean particle sizes of 0.5 and 0.4 μm, specific surface areas of 4.0 and 4.7 m<sup>2</sup> g<sup>−1</sup>, and densities of 8.3 and 6.0 g cm<sup>−3</sup>, respectively, were used as starting materials.

Zeta potentials of nickel (Ni) and stabilized zirconia (YSZ) suspensions were determined by laser Doppler velocimetry (Zetasizer NanoZS, Malvern, UK). For this purpose, suspensions of 0.1 g l<sup>−1</sup> of Ni and YSZ powders were prepared in a 10<sup>−3</sup>N KCl aqueous solution by ultrasonic mixing, using a 400 W sonication probe (Hielscher UP400S, Germany) for 2 min. According to a previous work<sup>7</sup> suspensions were prepared at pH > 9 adding tetramethylammonium hydroxide (TMAH). A commercial polyacrylic acid based polyelectrolyte (PAA, Duramax D-3005, Rohm and Haas, USA) was also employed as dispersant agent.

The rheology of aqueous suspensions of Ni/YSZ mixture (50/50, v/v) was evaluated under different dispersing conditions including the PAA at concentrations ranging from 0 to 5 wt.% and different pHs. The evolution of the suspension viscosity was measured using a rotational rheometer (Haake RS50, Germany) with a double cone–plate measurement system.

EPD experiments were performed in galvanostatic conditions using a power source AMEL (551, UK). Current densities up to 2 mA cm<sup>−2</sup> were applied during 5 and 10 min using Ni/YSZ suspensions. The addition of carboxymethylcellulose (CMC, OPTAPIX, Zschimmer-Schwarz, Germany) as a binder has been also studied. Commercial graphite foils (Carbonne Lorraine, France) were used as substrate and counterelectrode. Both electrodes were separated at a distance of 2 cm each other. The immersed area of the preform was 2.5 cm × 2.5 cm. EPD equipment was provided with a lift in order to assure a constant

\* Corresponding author. Tel.: +34 91 7355 840; fax: +34 91 7355 843.  
E-mail address: [bferrari@icv.csic.es](mailto:bferrari@icv.csic.es) (B. Ferrari).

withdrawal rate of  $7.5 \text{ mm s}^{-1}$ . The mass of each deposit was characterized by gravimetry after 48 h drying.

Phase identification was carried out by X-ray diffraction (XRD) using a Siemens D-5000 equipment (Germany). XRD patterns were made of both the powders attained from the dried slips, and the thick film cermet after the reducing heat treatment, in order to assure the total reduction of the NiO phase into metal.

Dynamic sintering tests were performed on bulk pieces obtained by casting the Ni, YSZ and mixture suspensions onto a plastic mold and further drying. A push-rod dilatometer (Netzsch, Germany) was used and experiments were performed under flowing  $\text{N}_2/10 \text{ vol.}\% \text{ H}_2$  atmosphere. Samples were treated up to  $1400^\circ\text{C}$  at a heating and a cooling rate of  $5^\circ\text{C}/\text{min}$ , and keeping a dwell time of 1 h.

Sintering schedule of green bodies included a two-step cycle in which samples were firstly treated at  $800^\circ\text{C}$  for 1 h in air to burn out the graphite and subsequently treated in a  $\text{N}_2/10 \text{ vol.}\% \text{ H}_2$  atmosphere at  $1200^\circ\text{C}$  for 1 h with heating and cooling rates of  $5^\circ\text{C min}^{-1}$ . Microstructural observations were made by scanning electron microscopy (SEM, Zeiss DSM-400, Germany).

### 3. Results and discussion

Fig. 1 shows the evolution of zeta potential of Ni and YSZ suspensions versus the polyelectrolyte concentration. Zeta potential measurements verify that the use of an anionic polyelectrolyte promotes the negative charging of particle surfaces, and hence deposition will take place in the anode. The absolute values of zeta potential of YSZ suspensions are larger than those of the Ni suspensions along the range of deflocculant concentrations considered. It increases with the addition of PAA up to 50 mV for additions higher than 1 wt.%. Similarly, Ni suspensions achieve a maximum zeta potential absolute value (35 mV) when the amount of PAA added exceeds 1 wt.%. In both cases, zeta potential maintains constant or tends to slightly decrease for further polyelectrolyte additions.

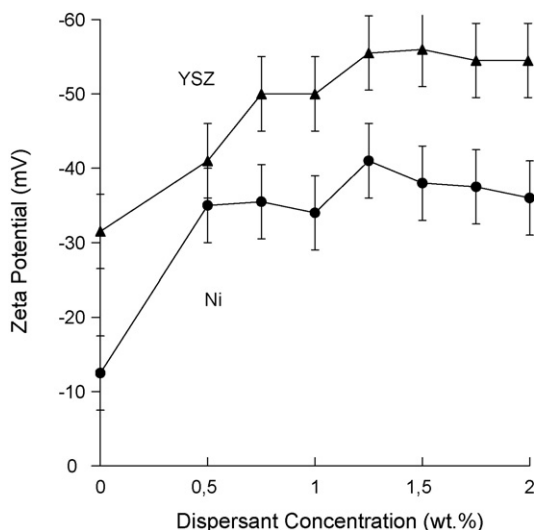


Fig. 1. Zeta potential evolution of  $0.1 \text{ g l}^{-1}$  YSZ and Ni suspensions with the PAA concentration.

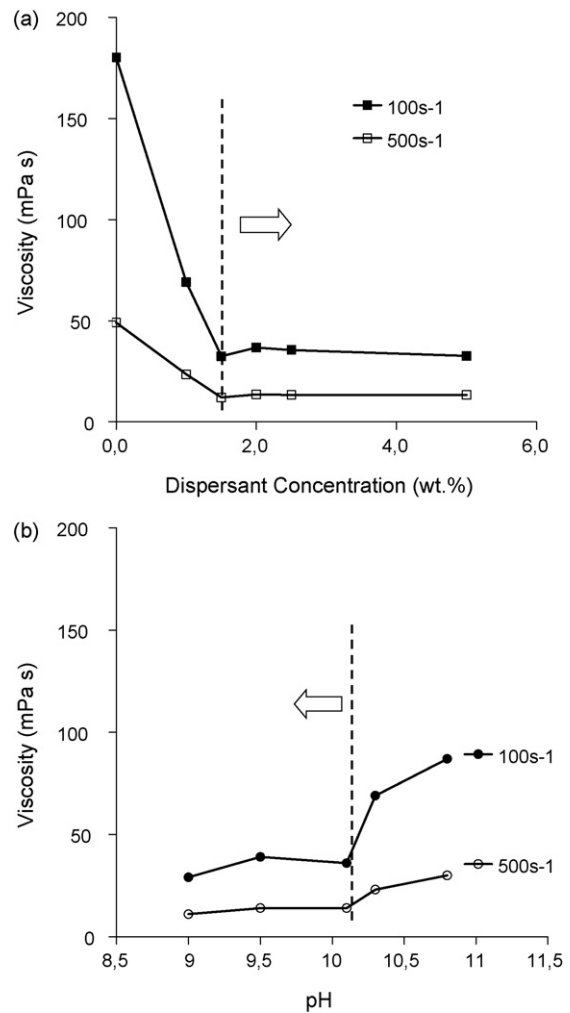


Fig. 2. Evolution of the viscosity of 10 vol.% 50 YSZ/50 Ni (v/v) suspensions vs. dispersant concentration (a) pH (b) at 100 and  $500 \text{ s}^{-1}$ . (a) Mixture prepared at pH 10 and (b) mixture prepared with 1.5 wt.% PAA.

The viscosity evolution of the Ni/YSZ mixture (50/50, v/v) prepared under different dispersing conditions by changing the PAA and TMAH concentration was studied. Fig. 2a and b show the viscosity values of 10 vol.% Ni/YSZ suspensions measured at 100 and  $500 \text{ s}^{-1}$ . Fig. 2a shows the variation of viscosity of suspensions prepared at pH 10 with the concentration of polyelectrolyte. The minimum viscosity value is achieved for suspensions deflocculated adding PAA  $\geq 1.5 \text{ wt.}\%$ .

The viscosity change of a 10 vol.% Ni/YSZ suspension prepared with 1.5 wt.% of PAA at different pH values is plotted in Fig. 2b. In this case, the suspension viscosity clearly increases when  $\text{pH} > 10$  as a consequence of the higher ions concentration in the medium, verifying that the most stable suspensions can be obtained adding 1.5 wt.% of PAA in a range of  $\text{pH} < 10$ .

Ni/YSZ suspensions were prepared for EPD tests at the optimum conditions. Deposition was performed applying current densities up to  $2 \text{ mA cm}^{-2}$  during 5 and 10 min. Fig. 3 shows the film growth in terms of deposited mass. The values collected at current density zero correspond to the samples obtained by dipping. For the 10 min tests the deposit growth is proportional

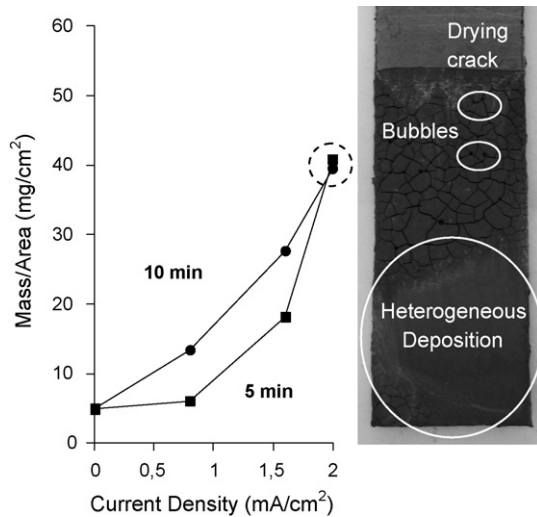


Fig. 3. Deposit growth vs. the applied current density for deposition times of 5 and 10 min. Picture of the film obtained applying  $2 \text{ mA cm}^{-2}$  for 10 min.

to the current density. However, for shorter tests (5 min) deposition begins for current densities higher than  $0.6 \text{ mA cm}^{-2}$ . The picture in Fig. 3 shows the sample obtained applying  $2 \text{ mA cm}^{-2}$  during 10 min. Under these conditions heterogeneous deposition takes place. The picture reveals the common heterogeneities promoted by a non-uniform coating of the substrate surface and the cracks formed during drying. Furthermore, current density was limited ( $<1.6 \text{ mA cm}^{-2}$ ) by the evident formation of defects due to the water electrolysis, as can be also seen in the picture.

CMC was used as a binder to improve EPD results. Fig. 4 plots the mass per unit area of deposits obtained by dipping and EPD, applying  $0.8$  and  $1.6 \text{ mA cm}^{-2}$  during 5 min, as a function of CMC content. Dipping did not improve with the addition of CMC. Deposits mainly grow by electrophoresis, being the heaviest ones those obtained from a suspension with  $0.5 \text{ wt.}\%$  of CMC at both current densities. Deposition with CMC led to uniform coatings, although they crack above a critical thickness ( $t_c$ ) occurring for a deposited mass higher than  $10 \text{ mg cm}^{-2}$ . In such aqueous system, the  $t_c$  depends on the in-plane developed stress and the coating toughness.<sup>8</sup> The addition of CMC improves the coating toughness while relaxes the capillarity stresses, and

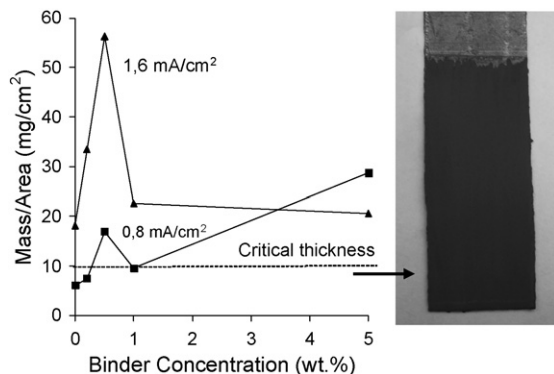


Fig. 4. Deposit growth vs. the binder concentration for an applied current density of  $0.8$  and  $1.6 \text{ mA cm}^{-2}$  and deposition times of 5 min. Picture of a film attained under the critical thickness conditions.

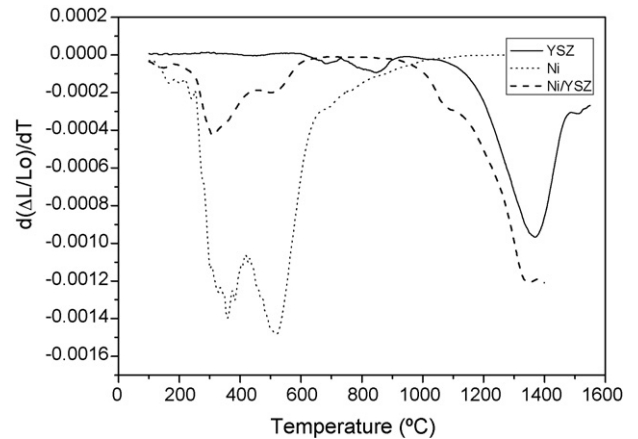


Fig. 5. Derivative of the shrinkage curves for the monoliths of Ni, YSZ and the mixture Ni/YSZ (50/50, v/v).

hence homogeneous and crack-free deposits with a mass per unit area of  $10 \text{ mg cm}^{-2}$  can be obtained.

Fig. 5 shows the derivative of the shrinkage curves registered for samples of Ni, YSZ and Ni/YSZ mixture (50/50, v/v) treated under a  $\text{N}_2/\text{vol.}\% \text{ H}_2$  atmosphere up to  $1400 \text{ }^\circ\text{C}$ . Ni shows two significant shrinkage stages at  $350$  and  $\sim 550 \text{ }^\circ\text{C}$ , which could correspond to the neck formation between particles and the structure densification, respectively. Both peaks appear at lower temperatures than those of monoliths prepared from larger Ni particle powders, described in previous works, in the same sintering conditions.<sup>9</sup> YSZ particles seem to start the necks formation between  $700$  and  $850 \text{ }^\circ\text{C}$ , reaching the highest shrinkage rate at  $1370 \text{ }^\circ\text{C}$ . The derivative of the shrinkage curve of the Ni/YSZ mixture sample shows the same peaks assigned to the earlier sintering stage of Ni ( $300\text{--}350 \text{ }^\circ\text{C}$ ), however those peaks associated to YSZ ( $700\text{--}850 \text{ }^\circ\text{C}$ ) appear slightly shifted to  $1050 \text{ }^\circ\text{C}$ , suggesting that sintering of the YSZ particles is retarded by the interposition of a Ni structure earlier developed. The final shrinkage of the mixture samples after heating at  $1400 \text{ }^\circ\text{C}$  is around  $35\%$ . Furthermore, during the dwell step the sintering yields a further shrinkage up to  $50\%$ . To sinter the Ni/YSZ layers, a temperature of  $1200 \text{ }^\circ\text{C}$  has been selected to allow the formation of YSZ necks through the Ni structure, leaving a porous microstructure.

YSZ (ASTM 30-1468) and metallic Ni (ASTM 04-0850) phases were detected after the thermal treatment. Since a reducing atmosphere was used, NiO phase was never detected after sintering.

The SEM microstructures of a cross-section and both film surfaces are shown in Fig. 6. The white, grey and dark areas represent the nickel, the YSZ, and the pores, respectively. A thick film of  $\sim 50 \mu\text{m}$  is produced. A uniform distribution of nickel in the cermet can be observed across the sample and at surface B. A monolayer of YSZ less than  $1 \mu\text{m}$  thick is formed at the surface of the sample that was in contact with the substrate during EPD (see surface A in the cross-section). This demonstrates that YSZ particles are the first to deposit when the electric field is applied because of their higher electrophoretic mobility (higher zeta potential in Fig. 1). As a consequence, the slip continuously

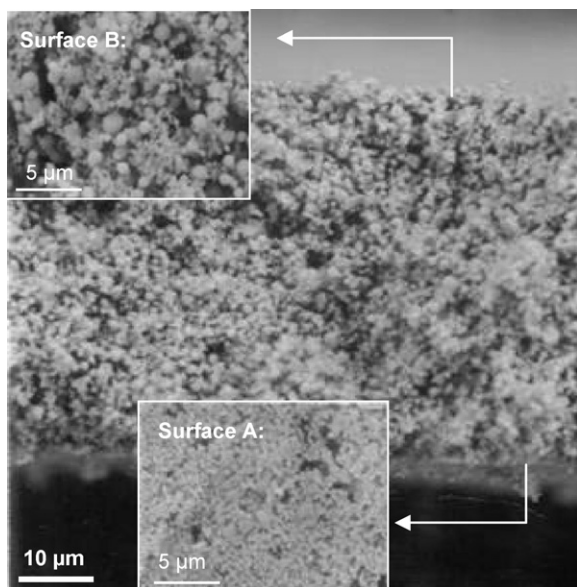


Fig. 6. SEM microstructure of a self-supported film cross-section. Details of the microstructure of the surfaces A and B.

changes its composition as YSZ is being deposited, and hence a functionally graded material can be produced in one step.

#### 4. Conclusions

The stability of 10 vol.% aqueous suspensions of Ni, YSZ and a mixture 50/50 (v/v) of both, was studied through zeta potential and viscosity measurements as a function of deflocculant contents and pH. Optimum dispersing conditions were obtained for pH between 9 and 10 adding 1.5 wt.% of PAA, leading to a higher electrophoretic mobility for YSZ powders. At these conditions EPD kinetics was too slow, and a high electric field was necessary to produce thick films, which led to bubbles and related

defects. The addition of 0.5 wt.% of CMC as a thickener allowed manufacturing homogeneous and crack-free YSZ/Ni-YSZ films with up to  $10 \text{ mg cm}^{-2}$  deposited mass.

Dynamic sintering, XRD and SEM studies reveal that it is possible to obtain by aqueous EPD self-supported graded films, composed by a thin YSZ layer ( $<1 \mu\text{m}$ ) and a porous thicker Ni/YSZ layer, taking advantage of the different mobility of Ni and YSZ particles.

#### Acknowledgment

This work has been supported by Ministerio de Educación y Ciencia (Spain) under contract MAT2003-00836.

#### References

1. Singhal, S. C., Science and technology of solid-oxide fuel cells. *MRS Bull.*, 1997, **25**(3), 16–21.
2. Will, J., Mitterdorfer, A., Kleinlogel, C., Perednis, D. and Gauckler, L. J., Fabrication of thin electrolytes for second-generation solid oxide fuel cells. *Solids State Ionics*, 2000, **131**(1/2), 79–96.
3. Sarkar, P. and Nicholson, P. S., Electrophoretic deposition (EPD): mechanisms, kinetics, and application to ceramics. *J. Am. Ceram. Soc.*, 1996, **79**, 1987–2002.
4. Negishi, H., Sakai, N., Yamaji, K., Horita, T. and Yokokawa, H., Application of electrophoretic deposition technique to solid oxide fuel cells. *J. Electrochem. Soc.*, 2000, **147**(5), 1682–1687.
5. Ferrari, B., de Francisco, I. M. and Moreno, R., Ni-YSZ self-supported films by gel electrophoresis. *Ceram. Int.*, 2005, **31**, 863–868.
6. Zhitomirsky, I. and Petric, A., Electrophoretic deposition of ceramic materials for fuel cell applications. *J. Eur. Ceram. Soc.*, 2000, **20**(12), 2055–2061.
7. Hernandez, N., Moreno, R. and Sanchez-Herencia, A. J., Surface behavior of nickel powders in aqueous suspensions. *J. Phys. Chem. B*, 2005, **109**(10), 4470–4474.
8. Kiennemann, J., Chartier, T., Pagnoux, C., Baumard, J. F., Huger, M. and Lamerant, J. M., Drying mechanisms and stress development in aqueous alumina tape casting. *J. Eur. Ceram. Soc.*, 2005, **25**, 1551–1564.
9. Ferrari, B., Sanchez-Herencia, A. J. and Moreno, R., Nickel–alumina graded coatings obtained by dipping and EPD on nickel substrates. *J. Eur. Ceram. Soc.*, 2006, **26**(12), 2205–2212.